Solving the System of Atomic Rate Equations During Recombination

by

Daniel Scolnic

Submitted to the Department of Physics
in partial fulfillment of the requirements for the degree of

Bachelor of Science in Physics

at the

MASSACHUSETTS INSTITUTE OF TECHNOLOGY

June 2007

Author .....
Department of Physics
May 11, 2007

Certified by .....
Edmund Bertschinger
Professor
Thesis Supervisor

Accepted by .....
David Pritchard
Department of Physics

Solving the System of Atomic Rate Equations During Recombination

by

Daniel Scolnic

Submitted to the Department of Physics
on May 11, 2007, in partial fulfillment of the
requirements for the degree of
Bachelor of Science in Physics

Abstract

The recombination of hydrogen at $z \sim 800 - 1800$ induces distortions to the Cosmic Microwave Background (CMB) spectrum. We present a careful calculation and analysis of all of the main transitions occuring during this period in order to find the electron density throughout recombination and its dependence on each process.

Our original motivation was to analyze the effects that Thomson scattering and resonance scattering will have on recombination. However, while working on the project, we found that first we had to thoroughly account for all of the atomic transitions. We present a new method for solving the system of equations throughout the period of recombination. This method allows us to show the effect of individual processes on the total ionization fraction.

Thesis Supervisor: Edmund Bertschinger
Title: Professor

Acknowledgments

Thanks to Prof. Bertschinger for allowing me to work with him and for being a great mentor to me these last four years. Also, thanks to Prof. Pritchard for taking the time to read this.

Contents

List of Figures

List of Tables

Chapter 1

Introduction

A simplistic model of the Cosmic Microwave Background (CMB) has two parts. 1) Early on, the photons, baryons and electrons were in thermal equilibrium in a hot dense plasma. The universe expanded and eventually the photons cooled enough that they could no longer keep hydrogen ionized. This process transforms the background plasma to a mainly neutral gas. 2) Since this decoupling the photons have been traveling unimpeded. These photons redshift to become the observed Cosmic Microwave Background (Scott & Smoot, 2004) and the effects of recombination can be seen in the observed properties of the CMB.

The basic physical picture for cosmological recombination has not changed since the early work of Peebles (1968) and Zel'dovich, Kurt and Sunyaev (1968). Peebles helped create a detailed understanding of the recombination process that is still one of the most important papers in the field . As the universe cools, it becomes matter dominated around $z \sim 10^4$. At $T \sim 4000$ K, the radiation is no longer able to maintain a high enough level of ionization to combine p^+ and e^- to form neutral H. While the ionization potential of H is 13.6 eV, which is equivalent to a temperature of $150,000$ K, the high-energy tail of the Planck function is still doing the ionization when the peak energy of the blackbody spectrum is below 13.6 eV.

There have been several refinements introduced since then, motivated by the increased emphasis on obtaining an accurate recombination history as part of the calculation of CMB anisotropies. There has been a stronger focus on the distortions of the

photon spectrum because of the large abundance of photons over baryons. Seager, Sasselov & Scott (1999,2000) expanded Peebles' and Zel'dovich's work and made very careful calculations of the effect of recombination on an atomic level. They showed that since the ratio of photons to baryons is so high, certain atomic transitions can distort the photon background which in turn can play a part in affecting the entire recombination process. They presented a detailed calculation of the whole recombination process, with no assumption of equilibrium among the energy levels. We hope to reproduce such a calculation with a new method for solving such that we can show the effect of each process on recombination.

Theoretical work done on this subject is so exciting at present because of the observational measurements taken recently. From the Far-Infrared Absolute Spectrophotometer measurements on the COBE satellite, Mather et al (1999) showed that the CMB is well modelled by a $2.725 \pm .001$ K blackbody, and that any deviation from this spectrum around the peak are less than 50 parts per million of the peak brightness. This fact is not only important for our calculations, but also shows that we are now in what many cosmologists call the era of precision cosmology.

Hence, we could safely expect the various distortions produced by theorizing a multi-level atom or looking at various collisional processes will be measured in near-future experiments. In fact, the PLANCK satellite, which has been designed to have ten times better instantaneous sensitivity and more than fifty times the angular resolution of COBE, should be able to pinpoint the effect of many of the main processes.

This means that a detailed understanding of the physics of recombination is crucial for calculating the distortion. The aim of this paper is to calculate all of the main hydrogen transitions during the era of recombination and show their effect on the electron ionization fraction of the universe. In chapter 2, we present the basic cosmology during the era of recombination as well as an overview of the transitions we will be studying. In chapter 3, we will calculate the bound-bound and bound-free processes and compare our findings to the Peebles paper. In chapter 4, we will present our methods for solving the atomic rate equations and in chapter 5, we will show our results. In chapter 6, we will discuss including Thomson and Resonance Scattering

into our equations and finally, we will present our conclusions in the last chapter.

Chapter 2

Basic Cosmology

2.1 Expansion of the Universe

Around $z \sim 10^4$,or $a = 1/(1+z) \approx 10^{-4}$, the universe becomes matter dominated, as we can see by the Hubble factor $H \equiv \dot{a}/a$

$$H(a)^2 = H_0{}^2 \left(\Omega_M a_{eq} a^{-4} + \Omega_M a^{-3} + \Omega_K a^{-2} + \Omega_\Lambda\right) \tag{2.1}$$

All the numerical results are made using the ΛCDM model, as given in Seager (1999), with parameters: $H_0 = 71$ km/s/Mpc $= 2.3 \times 10^{-18}$ s^{-1}; $\Omega_B = 0.046$; $\Omega_M = 0.3$; $\Omega_\Lambda = 0.7$; $\Omega_K = 0$; $a_{eq} = 5.1 \times 10^{-5}$; $T_0 = 2.725$ K. Here a_{eq} is the expansion factor when matter and radiation are of equal strength and T_0 is the present background temperature as discussed earlier.
Around $z \sim 1000$, the effect of the radiation density on the Hubble parameter is about 10% of the effect of the matter density so, like in Peebles calculation, we could approximate the universe as completely matter dominated.

Since later in the paper we will be comparing our transition rates against the Hubble rates, it is useful to plot the Hubble rate for the range of redshifts we are studying.

If the universe was complete ionized, the number density of electrons would depend

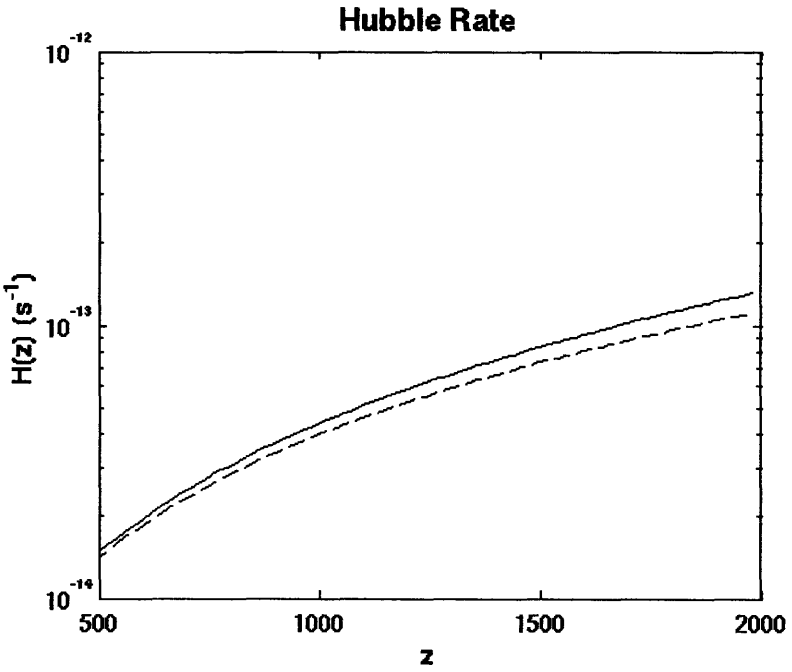

Figure 2-1: We show the Hubble rate given by Eqn. 2.1 as well as the rate assuming a matter dominated universe. The full Hubble rate is the higher curve.

on the redshift as

$$n_e = n_{0H}(1+z)^3 \tag{2.2}$$

where the number density of electrons today, $n_{0H} = 9.83\Omega_b h^2 m^{-3} = .2163\ m^{-3}$. To run our simulations, we must begin before the electron fraction drops noticeably below 1, which starts to happen around $z = 1800$.

The dependance of the photon temperature on redshift follows

$$T_\gamma = 2.725\,(1+z)\ K. \tag{2.3}$$

and the temperature of matter is coupled to the photon temperature as

$$(1+z)\frac{dT_m}{dz} = \frac{8\sigma_T U}{3H(z)m_e c}\frac{n_e}{n_e + n_H + n_{He}}(T_M - T_\gamma) + 2T_M \tag{2.4}$$

where $U = a_R T_R^4$, a_R is the radiation constant and σ_T is the Thompson scattering cross section. For our calculations, we ignore the difference between the temperature

of matter and radiation and assume the matter temperature equals that of radiation.

2.2 Summary of All Interactions

The protons and electrons are bathed in a radiation in which there are 10^9 more photons than baryons. The background radiation can be modelled fairly well by a blackbody ,

$$f(E,t) = f_0\left(E/T_\gamma\right) = \frac{1}{e^{E/kT_\gamma} - 1}. \tag{2.5}$$

If there are distortions to the blackbody, we can rewrite $f(E,t)$ as

$$f\left(E,t\right) = f_0\left(\frac{E}{T_\gamma\left(1+\Delta\right)}\right) \tag{2.6}$$

where $\Delta = \Delta(E,t)$. We can find the total distortion to the blackbody by looking at all of the processes taking place

$$\frac{df}{dt} - HE\frac{df}{dE} = \left(\frac{df}{dt}\right)_{SZ} + \left(\frac{df}{dt}\right)_{rs} + \left(\frac{df}{dt}\right)_{ff} + \left(\frac{df}{dt}\right)_{bf} + \left(\frac{df}{dt}\right)_{fb} + \left(\frac{df}{dt}\right)_{bb}, \tag{2.7}$$

where SZ: Sunyaev-Zel'dovich. rs: resonance scattering. ff: free-free bf: bound-free(photoionization). fb:free-bound(recombination). In Peebles calculations, he mainly looks at bound-free and free-free processes in his approximation.

We will first look at the bound-bound, bound-free and free-bound processes. While doing so, we will assume a perfect blackbody. After doing so, we will look at the remaining processes including the Sunyaev-Zel'dovich effect and resonance scattering, and discuss the effect they have.

Chapter 3

Bound-Bound and Bound Free Transitions

3.1 Overview

The bound-bound, bound-free, and free-bound transitions that we will be calculating can be summarized as:

1. Bound-bound transitions

    - Permitted (e.g. $2p \leftrightarrow 1s + \gamma$)
    - Forbidden (e.g $2s \leftrightarrow 1s + \gamma_1 + \gamma_2$)
    - Collisional (e.g. $2p \leftrightarrow 2s$)

2. Bound-free transitions

    - Recombination $(p + e \rightarrow (n, l) + \gamma)$
    - Photoionization to $((n, l) + \gamma \rightarrow p + e)$

3.2 Bound-Bound Permitted

3.2.1 Selection Rules

A hydrogen atom can only make a spontaneous transition from an energy state corresponding to the quantum numbers n', l', m' if the modulus squared of the associated dipole moment is nonzero,

$$d^2 = |\langle n,l,m\,|ex|\,n',l',m'\rangle|^2 + |\langle n,l,m\,|ey|\,n',l',m'\rangle|^2 + |\langle n,l,m\,|ez|\,n',l',m'\rangle|^2 \quad (3.1)$$

The spontaneous transitions between different energy levels of a hydrogen atom are only possible provided

$$l' = l \pm 1, \quad (3.2)$$

$$m' = m, m \pm 1 \quad (3.3)$$

These are termed the selection rules for electric dipole transitions. For example, using the wave-function of hydrogen in the 2p state and 1s state,

$$\langle 1,0,0\,|x|\,2,1,\pm 1\rangle = \pm\frac{2^7}{3^5}a_0 \quad (3.4)$$

$$\langle 1,0,0\,|y|\,2,1,\pm 1\rangle = i\frac{2^7}{3^5}a_0 \quad (3.5)$$

$$\langle 1,0,0\,|z|\,2,1,0\rangle = \sqrt{2}\frac{2^7}{3^5}a_0 \quad (3.6)$$

where a_0 is the Bohr radius. All of the other possible $2P \rightarrow 1S$ matrix elements are zero because of the selection rules. The modulus squared of the dipole moment for the $2P \rightarrow 1S$ transition takes the same value:

$$d^2 = \frac{2^{15}}{3^{10}}(ea_0)^2 \quad (3.7)$$

for $m = 0, 1, -1$. The transition rate is independent of the quantum number m so we should expect equal amounts of transitions to the $m = 0, 1, -1$ states. We can

apply the lesson that the transition rate is independent of m to all of our permitted bound-bound transitions

3.2.2 Bound-Bound Absorption

Bound-bound absorption is the process wherein an electron is pumped to an excited state by the absorption of a photon of appropriate energy. The 1 photon reaction we will be studying is:

$$\gamma + (n, l) \rightarrow (n', l') \tag{3.8}$$

The likelihood of this happening must be proportional to the number of photons available at the appropriate frequency. The rate per target multiplets is equal to the flux multiplied by the cross section. The flux should have units of $\#cm^{-2}s^{-1}$ and the cross section should have units of cm^2.

The photon number flux is given by

$$cfd^3p = \frac{I_\nu}{h\nu} d\nu d\Omega, \tag{3.9}$$

where

$$f = \frac{1}{h^3} \frac{1}{e^{\frac{h\nu}{kT_\gamma(1+\Delta)}} - 1}. \tag{3.10}$$

Since $p = h\nu/c$ and $d^3p = p^2 dp d\Omega$,

$$cfd^3p = \frac{1}{e^{\frac{h\nu}{kT_\gamma(1+\Delta)}} - 1} \frac{\nu^2}{c^2} d\nu d\Omega \tag{3.11}$$

We will have to be multiply the photon number flux by 2 because f denotes the phase space distribution for each spin or polarization state.

There is a distribution of frequency values for which a photon can induce the transition, with an associated probability distribution that can be plotted as a line profile, which itself integrates to one.

$$\int_0^\infty \phi(\nu)\, d\nu = 1 \tag{3.12}$$

Table 3.1: Oscillator strength f_{mn}

Final Level: n	m=1(Lyman)	m=2(Balmer)	Initial level m: m=3(Paschen)
1		-0.104	-0.0087
2	0.416		-0.284
3	0.079	0.637	
4	0.029	0.119	0.841
5	0.014	0.044	0.151
6	0.008	0.022	0.056

The cross section is then:

$$\sigma(\nu) = \frac{e^2}{4\epsilon_0 m_e c} f_{osc} \phi(\nu) \tag{3.13}$$

where f_{osc} is the oscillator strenth. $\frac{e^2}{4\epsilon_0 m_e c}$ has units of m^2/s, $\phi(\nu)$ has units of s so the entire cross section has units of m^2. This will then mean the flux multiplied by the cross section has units of $1/s$.

f_{mn} can be approximated by following useful formula given in Omidvar and McAllister, 1995,

$$f(m,n) \approx \frac{2^6}{6\sqrt{3\pi} m^5 n^5} \left[\frac{1}{m^2} - \frac{1}{n^2}\right]^{-3} F(m,n) \tag{3.14}$$

where

$$F(m,n) = 1 - .17286\frac{AB^{-2/3}}{m^{2/3}} - .0165\frac{AB^{-4/3}}{m^{4/3}} + \frac{1}{175}\frac{AB^{-2}C}{m^2} + O(1/m^{8/3}) \tag{3.15}$$

and $A = 1 + \alpha^2$, $B = 1 - \alpha^2$, $C = 3 - 4\alpha^2 + 3\alpha^4$, $\alpha = m/n$. f_{mn} is then given in the following table, which agrees to within .5% of the values posted by Menzel and Pekeris, 1935.

Finally the rate per target multiplet:

$$Rate = 2\int\int \frac{1}{e^{\frac{E}{kT_\gamma(1+\Delta)}} - 1} \frac{\nu^2}{c^2} \frac{e^2}{4\epsilon_0 m_e c} f_{osc} \phi(\nu)\, d\nu d\Omega \tag{3.16}$$

If we assume $\phi(\nu)$ acts as $\delta(\nu)$ then we have a rate of:

$$Rate = 8\pi \frac{1}{e^{\frac{E}{kT_\gamma(1+\Delta)}} - 1} \frac{\nu^2}{c^2} \frac{e^2}{4\epsilon_0 m_e c} f_{osc} \tag{3.17}$$

3.2.3 Bound-Bound Emission

For 1-photon Bound-Bound emission, there are spontaneous and stimulated transitions.

Spontaneous: $(n', l') \rightarrow (n, l) + \gamma$

Spontaneous emission is the process wherein an electron in an excited state spontaneously de-excites and emits a photon. Einstein used the principle of detailed balance (i.e., as many absorptions as emission), with assumptions about the transitions and comparison with the Planck law, to derive relations between the emission and absorption rates with time.

A_{nm} is the transition probability per unit time for spontaneous emission. A_{nm} is given in the equation:

$$g_{nm} A_{nm} = \frac{2h\nu^3}{c^2} \left(\frac{e^2 \pi}{\epsilon_0 m_e c h \nu} \right) f_{nm} \tag{3.18}$$

1-photon bound-bound emission produces line profile $\phi(\nu)$. The rate of photons with freq. in $\nu + d\nu$ is $A_{nm}\phi(\nu)\, d\nu \times n_{mp}$ where n_{mp} is the number of atoms in the upper level.

Stimulated: When Einstein equated the above absorption and emission processes, he could not derive a form for the emission consistent with the Planck Law. To do this, he had to add an additional term which accounted for emission processes that were stimulated by interaction with a photon.

$B_{21}\overline{J}$ =The transition probability per unit time for stimulated emission. where

$$\overline{J} = \int_0^\infty \overline{I}_\nu \phi(\nu)\, d\nu \tag{3.19}$$

and $J_\nu = \int \overline{I_\nu} d\Omega / (4\pi)$. As discussed earlier, for very narrow line profiles, $\overline{J} \sim J_\nu$.

To derive the Einstein relations, we will use the first and second states and all the terms for emission and absorption and put them into an expression which equates the emission and absorption processes (i.e. Kirchoff's Law):

$$n_1 B_{12} \overline{J} = n_2 A_{21} + n_2 B_{21} \overline{J} \tag{3.20}$$

Re-arranging these to solve for the emission intensity, J-bar gives:

$$\overline{J} = \frac{\frac{A_{21}}{B_{21}}}{\frac{g_1 B_{12}}{g_2 B_{21}} e^{\frac{h\nu}{kT}} - 1} \tag{3.21}$$

Now this equation has the same form as Planck's Law. Equating them yields the Einstein Relations:

$$g_1 B_{12} = g_2 B_{21} \tag{3.22}$$

$$A_{21} = \frac{2h\nu^3}{c^2} B_{21} \tag{3.23}$$

These equations relate microscopic inverse processes under equilibrium and are also known as the "Detailed Balance Relations". Principle of Detailed Balance: In equilibrium, the rate of every process equals the rate of the corresponding inverse process.

Using the Einstein relation between A_{21} and B_{21}, to obtain B_{21} from A_{21} we multiply the spontaneous rate by $n(\nu)$ where $n(\nu)$ is the number density of the photons (not a blackbody).

Rate of photons $\Rightarrow$ spontaneous + stimulated is then

$$Rate_{sp,st} = n_2 A_{21} \phi(\nu) \, d\nu \, (1 + n_\gamma) \tag{3.24}$$

so if we assume $\phi(\nu)$ acts like a delta function,

$$R_{nm} = A_{nm}(1 + n_\gamma). \tag{3.25}$$

Table 3.2: Rate coefficient $A_{mn}(s^{-1})$

Final Level: n	$m = 1$(Lyman)	$m = 2$(Balmer)	Initial level m: $m = 3$(Paschen)
1			
2	4.67×10^8		
3	5.54×10^7	4.39×10^7	
4	1.27×10^7	8.37×10^6	8.94×10^6
5	4.10×10^6	2.52×10^6	2.19×10^6
6	1.64×10^6	9.68×10^5	7.74×10^5

$$A_{mn} = \frac{g_n}{g_m}\left(\frac{2\nu_{mn}^2}{c^3}\right)\left(\frac{e^2\pi}{\epsilon_0 m_e}\right) f_{mn} \tag{3.26}$$

where ν_{mn} is the frequency of the transition.

We can see a table of A_{nm} for levels $n = 1$ to $n = 6$. This table shows the rates going from atomic level to another, without an l dependence. Our calculations include the l dependence.

Let us remember now that n_γ is dependent on the frequency and allows for a deviation from the blackbody:

$$n_\gamma(\nu, t) = \left[e^{h\nu/kT(1+\Delta)} - 1\right]^{-1}, \quad \Delta = \Delta(\nu, t) \tag{3.27}$$

To make our expression we simpler, we let

$$A_{mn} = K\frac{g_n}{g_m}(1/n^2 - 1/m^2)^2 f_{mn} \tag{3.28}$$

where $K = \left(\frac{2\nu_1^2}{c^3}\frac{e^2\pi}{\epsilon_0 m_e}\right)$ and ν_1 is the frequency of the ground state energy level transition to the continuum.

For the case of A_{21}, $g_1 = 2$, $g_2 = 6$ and therefore

$$A_{21} = K \times 1/3 \times \frac{9}{16} \times f_{21} = \frac{3}{16}K f_{21} \tag{3.29}$$

$$R_{2p1s} = \frac{3}{16}K f_{21}(1 + n_\gamma)n_{2p} \tag{3.30}$$

Now, $f_{12} = -\frac{g_2}{g_1}f_{21}$, so therefore, comparing B_{12} to A_{21} we agree with the Einstein

relation

$$A_{21} = \frac{g_2}{g_1}\frac{2h\nu_{21}^3}{c^2}B_{12} \tag{3.31}$$

and we can express

$$R_{1s,2p} = \frac{g_2}{g_1}A_{21}n_\gamma = \frac{9}{16}Kf_{21}n_{1s}n_\gamma \tag{3.32}$$

where K and n_γ are given above.

We can check this by using detailed balance in equilibrium:

$$\frac{3}{16}K(1+n_\gamma)n_{2p}f_{21} = \frac{9}{16}Kf_{21}n_{1s}n_\gamma \tag{3.33}$$

In equilibrium, $n_\gamma = \frac{1}{e^x-1}$ and $\frac{n_\gamma}{1+n_\gamma} = e^{-x}$, $n_{2p}/n_{1s} = 3e^{-x}$, and using these two relations, this expression holds.

Therefore, for the lyman-alpha transitions, the total rate we have is:

$$\begin{aligned} R_{\text{Lyman }\alpha} = &+ \frac{3}{16}K(1+n_\gamma)f_{21}n_{2p} \\ &- \frac{9}{16}Kf_{21}n_\gamma n_{1s} \end{aligned} \tag{3.34}$$

where $K = \frac{2\nu_1^2}{c^3}\left(\frac{e^2\pi}{\epsilon_0 m_e c}\right)$.

3.2.4 Peebles Assumptions

The total rate of states per time and volume changing due to bound-bound emission is given by

$$\Delta R_{ml,1s} = A_{mp,1s}(1+n_\gamma)n_{ml}. \tag{3.35}$$

Peebles(Eq. 19) states that

$$n_{ml} = n_{2s}(2l+1)e^{-(E_2-E_m)/kT} \tag{3.36}$$

where $l = 1$ for all p orbitals, $B_2 = 3.4$ eV, and B_m is the binding energy of hydrogen in the m^{th} principal quantum number. In this picture, only the population of the ground state of the atom is out of equilibrium with all other bound states. We should

note now that while we will not be using this expression, it will allow us to check our results. Remembering 3.28, we can check the transition rate for each p state of the hydrogen levels to the $1s$ state, for $k \geq 2$,

$$R_{mp,1s} = K(1 - 1/m^2)^2 f_{m1} \times e^{-(E_2 - E_m)/kT}(1 + n_\gamma)n_{2s} \tag{3.37}$$

From the transition rate given by Eq. 3.28

$$R_{1s,mp} = \frac{g_m}{g_1} A_{m1} n_\gamma n_{1s} = K(1 - 1/m^2)^2 f_{m1} n_\gamma n_{1s} \tag{3.38}$$

Therefore the total rate of $1s \leftrightarrow mp$ is:

$$R = K(1 - 1/m^2)^2 f_{m1} \left(e^{-(E_2 - E_m)/kT}(1 + n_\gamma)n_{2s} - n_\gamma n_{1s} \right) \tag{3.39}$$

Let's check this using detailed balance

$$e^{-(E_2 - E_m)/kT}(1 + n_\gamma)n_{2s} = n_\gamma n_{1s} \tag{3.40}$$

Now $n_\gamma/(1 + n_\gamma) = e^{-(E_2 - E_m)/kT}$ so if $n_{1s} = n_{2s}$ in equilibrium then this expression holds true.

For our calculations, we will be using Eqn. 3.17 for bound-bound absorption and Eqn. 3.18 for bound-bound emission. We will be able to check our state populations with the Peeble approximations.

3.3 Bound-Bound Forbidden

The equation for two photon decay, $2s \leftrightarrow 1s + \gamma_1 + \gamma_2$, is given by

$$R^{\mathrm{H}}_{2s,1s} = \Lambda_{\mathrm{H}} \left(n^{\mathrm{H}}_{2s} \right). \tag{3.41}$$

where $\Lambda_{\mathrm{H}} = 8.23 s^{-1}$. While this rate is much slower than the Lyman-alpha rate, Peebles states that it is the two-photon rate that is the dominant rate during recom-

Table 3.3: Gaunt factor g_{bf}

Level: n,l	n_{1s}	n_{2s}	n_{2p}	n_{3s}	n_{3p}	n_{3d}	n_{4s}	n_{4p}	n_{4d}	n_{4f}
g_{bf}	.7973	.9346	.8567	.1062	.1098	.7626	.1179	.1246	.1131	.6034

bination. Here we are neglecting two-photon absorption.

3.4 Photoionization and Direct Recombination

The Photoionization cross section is given by:

$$\sigma_P = (\alpha_{EM} a^2) \frac{64\pi}{3\sqrt{3}} \frac{g_{bf}}{n^5} (\frac{\nu_\infty}{\nu})^3 \tag{3.42}$$

where $a = .529 \times 10^{-10}$ m, $\alpha_{EM} = 1/137.04$, $h\nu_\infty = 13.6$ eV and g_{bf} is the bound-free gaunt factor given in the following table.

The gaunt factor has a ν dependence so it should not be constant but we took the values at ionization threshold, which should be a valid approximation. These values were taken from Karzas and Latter, 1961. The rate for photoionization is then

$$\begin{aligned} R_P &= \int_{\nu_\infty}^{\infty} \frac{4\pi J(\nu)}{h\nu} \sigma_P d\nu \\ &= \frac{8\pi}{c^2} (\alpha_{EM} a^2) \frac{64\pi}{3\sqrt{3}} \frac{g_{bf}}{n^5} (\nu_\infty)^3 \int_{\nu_\infty}^{\infty} \frac{n_\gamma(\nu)}{\nu} d\nu \end{aligned} \tag{3.43}$$

For photoionization from 2s or 2p, $h\nu_\infty = 3.4$ eV. In figure 3-1, we show photoionization rates for the lower atomic levels during recombination.

The recombination rate is given by

$$R_{1s} = \alpha_s n_e n_p \tag{3.44}$$

We can use the Milne relation (Peebles, 1993) that

$$\frac{\sigma_\alpha}{\sigma_P} = \frac{2p_\gamma^2}{p_e^2} = \frac{2\hbar^2\omega^2}{c^2 p_e^2} \tag{3.45}$$

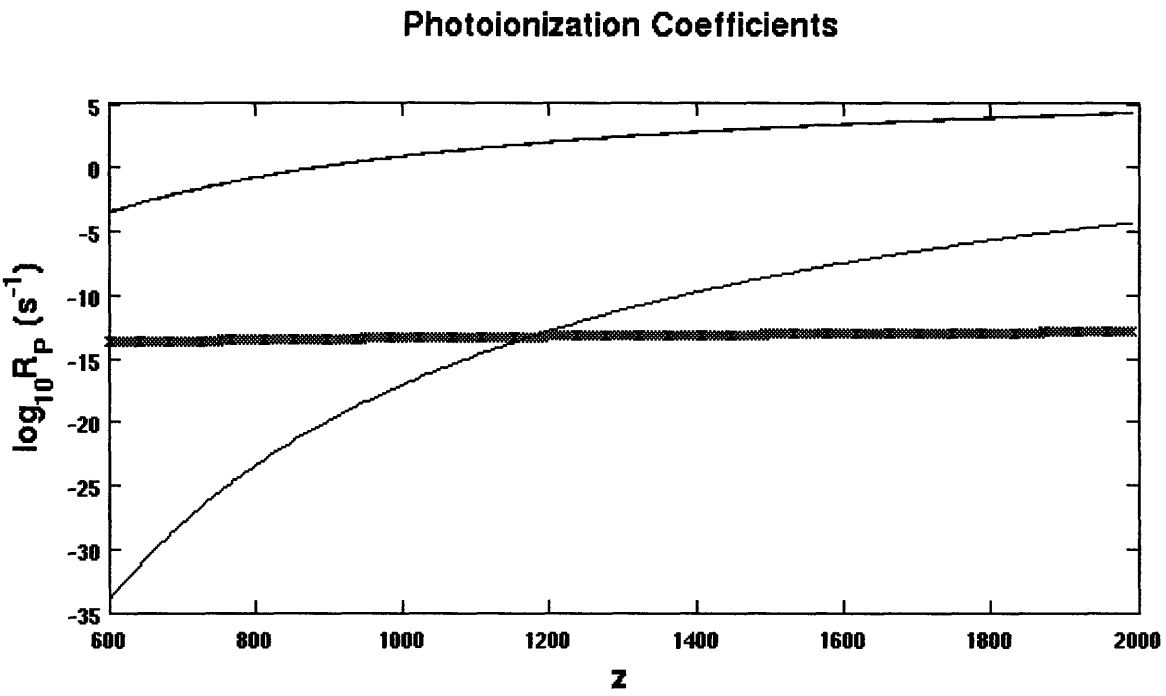

Figure 3-1: We show the photoionization rates for n_{1s} (bottom), n_{2s} and n_{2p} (top). The rates for n_{2s} and n_{2p} are extremely close, while n_{1s} drops off significantly, past the Hubble rate (shown by 'x').

to find the recombination coefficient α which is the product of the electron capture cross section and the electron velocity, averaged over a thermal distribution (Peebles, 1993).

$$\alpha = (2l+1)\int \frac{4\pi p^2 dp e^{-p^2/2mkT}}{(2\pi mkT)^{3/2}} \frac{p}{m} \frac{2\hbar^2\omega^2}{c^2p^2} \frac{\sigma_1\omega_1^3}{\omega^3} \tag{3.46}$$

The first factor here is the normalized probability distribution in the electron momentum. The photon energy is simply the sum of the electron kinetic energy and the hydrogen atom binding energy χ_1/n^2 such that $h\omega = p^2/2m + \chi_1$ and $\chi_1 = 13.6eV$. So finally,

$$\alpha = (2l+1)\frac{8\pi\sigma_1\chi_1^3 e^{\chi_1/(kTn^2)}}{(2\pi mkT)^{3/2}c^2}\int_{\chi_1/(kTn^2)}^{\infty} \frac{dx}{x}e^{-x} \tag{3.47}$$

If χ_1 is large compared to kT, the integral can be reasonable well approximated by e^{-x}/x.

This would give, for the ground state,

$$\begin{aligned} \alpha &= \frac{8\pi\sigma_P h^3 kT}{(2\pi mkT)^{3/2}c^2\chi_1} \\ &= \frac{2.07\times10^{-13}}{T_4^{1/2}}\mathrm{cm}^3\mathrm{s}^{-1} \end{aligned}$$

where $T = 10^4 T_4$ K. Peebles used this approximation in his calculations. He did not include the bound-free gaunt factor and we should note that at $T = 10000$ K, this expression has an accuracy within five percent. Also, it includes only recombinations to the ground state. From detailed balance, if we are in equilibrium, we have:

$$\alpha = \frac{8\pi P_c}{c^2}\int_{\nu_p}^{\infty}\frac{n_{BB}(\nu)}{\nu}d\nu \times \frac{n_{1s}}{n_e n_p} \tag{3.48}$$

Peebles also refers to the recombination coefficients from "Radiative Recombination Coefficients of the Hydrogen Atom", by W.J. Boardman (1964). Boardman only gives four values for recombination coefficients in our temperature range of interest to interpolate for each atomic level. We also found one more temperature value from Osterbrock, 1992, that matches the first three temperature values. These values are at $T = 1000$ K, $T = 3000$ K, $T = 5000$ K, and $T = 10000$ K. We fit a cubic solution to each set of four points. We plot our values as well as Boardman's in Figure 3-2. We can see that the two sets of values match up very nicely, with at most a 5% error.

3.5 Collisional Transitions

In "On the Effect of Collisional Transitions on the Cosmological Hydrogen Recombination Spectrum", Burgin, Kauts, and Shakhvorostova (2006) study the effect of collisional $2s \leftrightarrow 2p$ transitions on the populations of the $2s$ and $2p$ states at the cosmological hydrogen recombination epoch and on the intensity of the recombination $H\alpha$ line. They show that the relative change in the cosmological $H\alpha$ line intensity due to collisional transitions does not exceed 10^{-3}. We will be able to test this conclusion.

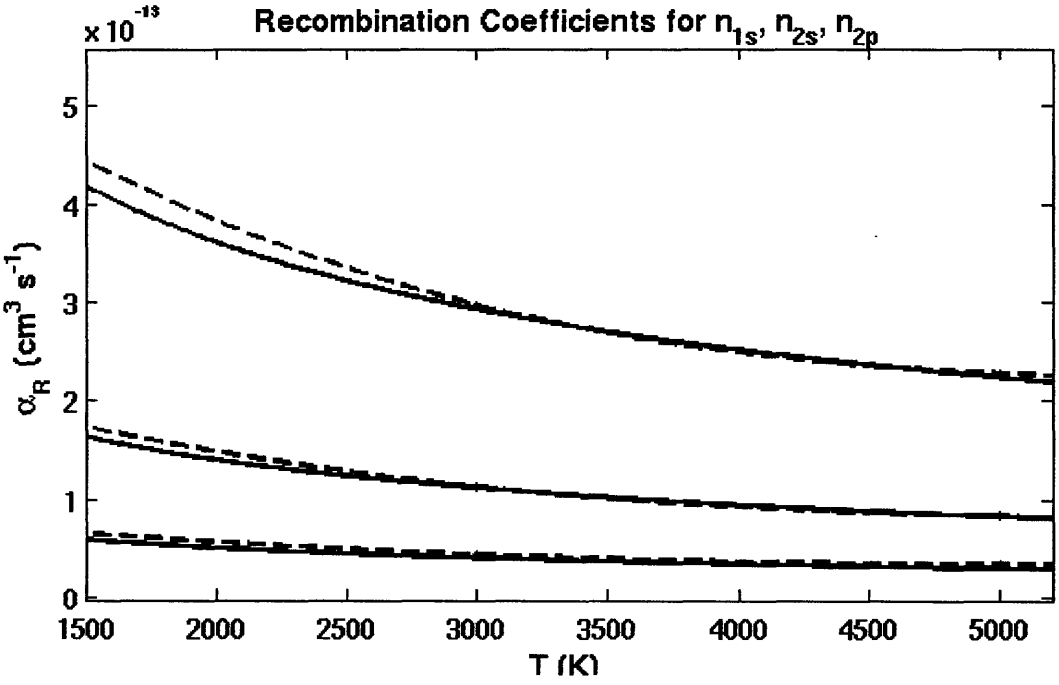

Figure 3-2: We show the recombination coefficents as predicted by Boardman (dashed line), and by Eqn. 3.47 (line). The topmost pair of curves show $\alpha_{n_{1s}}$, followed by $\alpha_{n_{2p}}$ and then $\alpha_{n_{2s}}$ at the bottom. We see a very strong correlation between our coefficients and Boardman's.

Burgin assumes a purely hydrogen plasma that recombines in a thermal radiation field. The plasma kinetic temperature and the radiation temperature are assumed to be equal, an assumption that we also hold. They find the collisional transition rate coefficients from previous studies that calculate the transition probability when an isolated hydrogen atom in the $2s$ state collided with a charged particle in the straight-path approximation. The probability that the $2s \rightarrow 2p$ transition will occur was calculated in a quantum mechanical way.

They find that

$$R_{2s,2p} = \frac{1.81 \times 10^{-4}}{\sqrt{T}} (\ln(T) + 2.83)\, cm^3 s^{-1} \times n_e \tag{3.49}$$

and from detailed balance

$$R_{2p,2s} = 3 \times \frac{1.81 \times 10^{-4}}{\sqrt{T}} (\ln(T) + 2.83)\, cm^3 s^{-1} \times n_e \tag{3.50}$$

3.6 Overall Equations

We show now the overall equations we will use for certain states. Compiling the equations for each state is necessary for solving the system of equations with our method.

- Overall equation for $1s$.

$$\begin{aligned} \frac{dn_{1s}}{dt} = & + \sum A_{kl,1s}(1 + n_\gamma) n_{kl} \\ & - \sum A_{kl,1s} n_\gamma \frac{g_{kl}}{g_1 s} n_{1s} \\ & + \Lambda_{\mathrm{H}} n_{2s} \\ & + \alpha_{1s} n_e n_p \\ & - R_P n_{1s} \\ & - 3H n_{1s} \end{aligned}$$

The rates for each line of the equation at $T = 3000K$ above are: $10^8\ s^{-1}$, $10^{-10}\ s^{-1}$, $8\ s^{-1}$, $10^{-13}\ s^{-1}$, $10^{-15}s^{-1}$, $10^{-15}s^{-1}$.

- Overall equation for n_{2s}.

$$\begin{aligned}\frac{dn_{2s}}{dt} = &+ \sum A_{kl,2s}(1+n_\gamma)n_{kl} \\ &- \sum A_{kl,2s}n_\gamma \frac{g_{kl}}{g_2 s} n_{2s} \\ &- \Lambda_{\mathrm{H}} n_{2s} \\ &+ \alpha_{2s} n_e n_p \\ &- R_P n_{2s} \\ &+ R_{2p,2s} n_{2p} \\ &- R_{2s,2p} n_{2s} \\ &- 3Hn_{2s}\end{aligned}$$

- Overall equation for n_p

$$\begin{aligned}\frac{dn_p}{dt} = &- \sum \alpha_{kl} n_e n_p \\ &+ \sum R_{P_{kl}} n_{kl} \\ &- 3Hn_p\end{aligned}$$

These are the overall equations for three states. Of course, there are many more states, and we will have to collect equations in a similar fashion for all of them. The majority of our states will have permitted bound-bound absorption, emission as well as photoionization and recombination.

3.7 Rate Equations from Wong, Seager,Scott

We can compare our equations to those presented in the paper *Spectral distortions to the Cosmic Microwave Background from the recombination of hydrogen and helium*, by Wong, Seager, and Scott.

They present a system of four differential equations.

$$(1+z)\frac{dn_1^{\rm H}(z)}{dz} = -\frac{1}{H(z)}[\Delta R^{\rm H}_{\rm 2p-1s} + \Delta R^{\rm H}_{\rm 2s-1s}] + 3n_1^{\rm H}; \tag{3.51}$$

$$(1+z)\frac{dn_2^{\rm H}(z)}{dz} = -\frac{1}{H(z)}[n_{\rm e}n_{\rm p}\alpha_{\rm H} - n^{\rm H}_{\rm 2s}\beta_{\rm H} - \Delta R^{\rm H}_{\rm 2p-1s} - \Delta R^{\rm H}_{\rm 2s-1s}] + 3n_2^{\rm H}; \tag{3.52}$$

$$(1+z)\frac{dn_{\rm e}(z)}{dz} = -\frac{1}{H(z)}\left[n^{\rm H}_{\rm 2s}\beta_{\rm H} - n_{\rm e}n_{\rm p}\alpha_{\rm H}\right] + 3n_{\rm e}; \tag{3.53}$$

$$(1+z)\frac{dn_{\rm p}(z)}{dz} = -\frac{1}{H(z)}\left[n^{\rm H}_{\rm 2s}\beta_{\rm H} - n_{\rm e}n_{\rm p}\alpha_{\rm H}\right] + 3n_{\rm p}. \tag{3.54}$$

Here the values of n_i are the number density of the ith state, where $n_{\rm e}$ and $n_{\rm p}$ are the number density of electrons and protons respectively. $\Delta R^{\rm H}_{i-j}$ is the net bound-bound rate between state i and j and the detailed form of $\Delta R^{\rm H}_{\rm 2p-1s}$ and $\Delta R^{\rm H}_{\rm 2s-1s}$ will be discussed in the next subsection.

$\Delta R^{\rm H}_{\rm 2p-1s}$ is the net rate of photon production between the 2p and 1s levels, i.e.

$$\Delta R^{\rm H}_{\rm 2p-1s} = p_{12}\left(n^{\rm H}_{\rm 2p}R_{21} - n_1^{\rm H}R_{12}\right). \tag{3.55}$$

Here $n_i^{\rm H}$ is the number density of hydrogen atoms having electrons in state i, the upward and downward transition rates are

$$R_{12} = B_{12}\bar{J}, \tag{3.56}$$

$$\text{and} \quad R_{21} = \left(A_{21} + B_{21}\bar{J}\right), \tag{3.57}$$

with A_{21}, B_{12} and B_{21} being the Einstein coefficients and p_{12} the Sobolev escape probability, which accounts for the redshifting of the Lyα photons due to the expansion of the Universe.

The only real difference between how we compute the $n_{2p} \leftrightarrow n_{1s}$ transition is their Sobolev escape probability.

This Sobolev escape probability should not play that much of a difference. At $z = 1800$, the probability is .998, so it has a negligible effect, and drops down to .002 at $z = 1200$. However, while this will make the rate A_{21} smaller, it is still so high (10^8 s^{-1}) compared to the rates, that the overall effect will not be diminished.

They assume a blackbody and include the difference between matter temperature and photon temperature, as given in Eq. (2.4). Seager states that this addition will only begin to have an effect at small redshifts. The hubble rate given, $3H$ is included within our rate equations.

In figure 3.7, we can see the results of the program RECFAST, which is a fortran code based on Seager et. al's method.

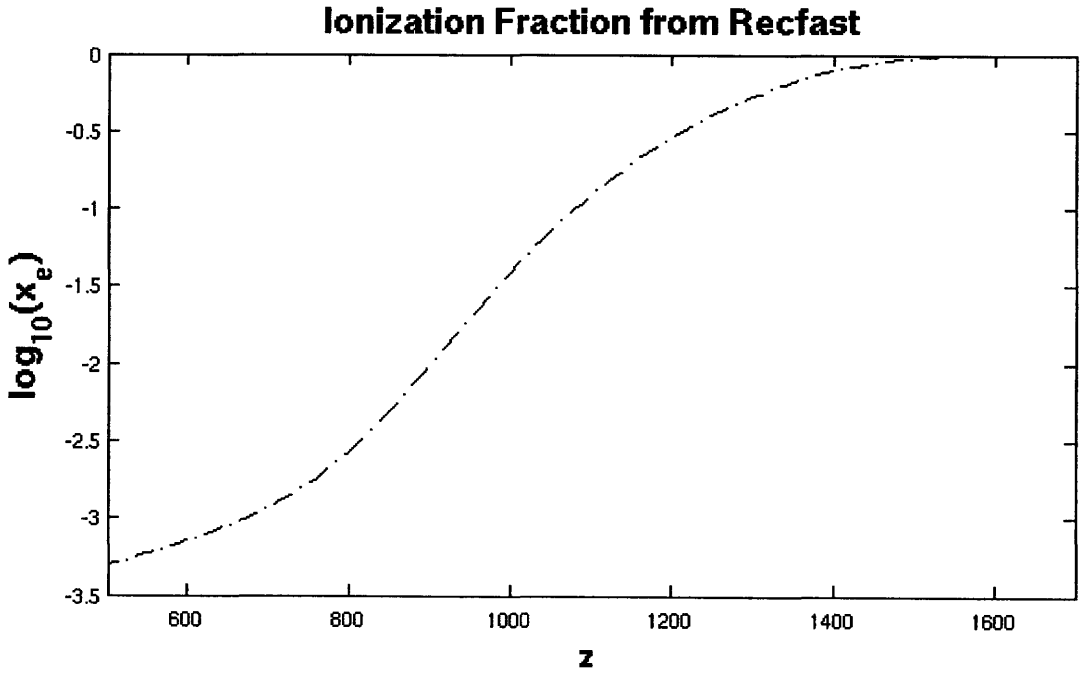

Figure 3-3: We show the ionization fraction x_e with redshift produced by RECFAST.

Wong, Seager and Scott, however, do not include many of the processes that we include. They only have photoionization from the n_{2s} state and state that recombination only affects the n_{2s} state, because of a boltzmann distribution with the other states. They do not include any atomic levels past $n = 2$ but make up for that using a Case B recombination coefficient. Also, they do not include the $n_{2p} \leftrightarrow n_{2s}$ collisions.

While several of their approximations hold just as well as our approach, our

method allows us to understand the effects of the individual processes. We will also be able to test their various approximations.

It is worth mentioning now that there are certain processes that neither these authors or we are looking at. We are not looking at two photon emission or absorption from $3s, 4s, 5s \ldots \leftrightarrow 2s$.

Also, we are not looking at free-free processes, and the only collisional process we are looking at is the one between $2s$ and $2p$.

We are now ready to discuss our method for solving the system of rate equations.

Chapter 4

Solving the Atomic Rate Equations

To understand how to solve the atomic rate equations, let us first look at a system with only the lyman-alpha transition,

$$\begin{aligned} \frac{dn_{1s}}{dt} &= +A_{21}n_{2p} - B_{12}n_{1s} \\ \frac{dn_{2p}}{dt} &= -A_{21}n_{2p} + B_{12}n_{1s}. \end{aligned} \tag{4.1}$$

This system has the general form,

$$\begin{aligned} \tfrac{dx}{dt} &= -Ax + By \\ \tfrac{dy}{dt} &= Cx - Dy \end{aligned} \tag{4.2}$$

which we can convert to

$$\frac{d}{dt}\begin{pmatrix} x' \\ y' \end{pmatrix} = \begin{pmatrix} -\alpha & 0 \\ 0 & -\beta \end{pmatrix}\begin{pmatrix} x' \\ y' \end{pmatrix}. \tag{4.3}$$

In many of our rate equations, the rate in one direction is much faster than the other. In the lyman-alpha transition, the emission rate is a factor of $1/n_\gamma$ greater than the absorption rate.

$$\frac{x'}{y'} = \frac{x'(0)}{y'(0)}e^{-(\alpha-\beta)} \to 0 \tag{4.4}$$

While Peebles assumes that there is thermal equilibrium, that one of the transitions is rapid, and that the photon spectrum is a blackbody, we will only assume that the process is rapid and not there there is thermal equilibrium. Eliminating one variable from our system of coefficients, we obtain the relationship between n_{2p}/n_{1s},

$$\frac{\frac{g_{2p}}{g_{1s}} n_{\gamma(\nu_{21})}}{1 + n_{\gamma(\nu_{21})}} = \frac{n_{2p}}{n_{1s}}. \tag{4.5}$$

Similarly, if Lyman-β is very rapid,

$$\frac{\frac{g_{3p}}{g_{1s}} n_{\gamma(\nu_{31})}}{1 + n_{\gamma(\nu_{31})}} = \frac{n_{3p}}{n_{1s}} \tag{4.6}$$

and therefore

$$\frac{n_{3p}}{n_{2p}} = \frac{n_\gamma(\nu_{31})}{1 + n_\gamma(\nu_{31})} \frac{1 + n_\gamma(\nu_{21})}{n_\gamma(\nu_{21})} \tag{4.7}$$

We can use this approximation instead of Peebles' approximations, and can check Peebles by assuming $n_\gamma = (e^{h\nu/kT} - 1)^{-1}$.

Now, any process that goes fast will cause an equilibrium, however, the pairs must go fast compared to the Hubble time. If they do not, there will be a disparity. We see that past certain redshifts, the absorption rate is below the Hubble rate while the emission rate is still well above it.

We must note also that the blackbody gives an understimate of the rate. If the rate is fast with a blackbody then for sure it will be fast with more photons.

Our general strategy is to make a matrix of all of our atomic levels, and to compare our fast processes with our slow processes. Certain processes might start out being rapid, but since the # of photons goes down, the rates will decrease. We will leave n_γ constant during one time step. Once we diagonalize, we will make the fast ones go to equilibrium, and only retain small ones. In future work, we will need to treat the photons as their own separate equations and employ the Kompaneets equation. The Kompaneets equation will constantly take photons in and out of bins. We will also then still need Thomson scattering, which should fix the photon spectrum and could wash out spectral features.

The first step is then to make a matrix, C, containing all of the transition rates. It will include all of the bound-bound, bound-free and free-bound transitions. We will let A_{ul} be the decay rate per upper atom including stimulated emission and B_{lu} be the absorption rate per lower atom including photon abundance. A_{ul} and B_{lu} have units of s^{-1}. Let β_i photoionization rate per atom in state i; $\alpha_i n_e$ is the recombination rate per proton to state i;

The matrix should be formed such that the matrix element $C_{i,j}$ should hold the transition rate producing state i from state j. For example, if we are looking at a matrix with only n_p, n_{1s} and n_{2p} , we should have the following entries for C.

$$\begin{pmatrix} -\alpha_{n_{1s}} n_e - \alpha_{n_{2p}} n_e & \beta_{n_{1s}} & \beta_{n_{2p}} \\ \alpha_{n_{1s}} n_e & -\mathrm{B}_{1s,2p} - \beta_{n_{1s}} & \mathrm{A}_{2p,1s} \\ \alpha_{n_{2p}} n_e & \mathrm{B}_{1s,2p} & -\mathrm{A}_{2p,1s} - \beta_{n_{2p}} \end{pmatrix}$$

The first row and column correspond to n_p, the second row and column correspond to n_{1s} and the last to n_{2p}. This matrix has the important property that all of the elements in each column add up to 0. This signifies that the total number of protons is conserved. If the rows, or columns, are linearly dependent, then the determinant is 0. This means the matrix should have at least one eigenvalue equal to 0.

We will make this C matrix but with a more complete account of the atomic levels. We will let N be a column vector whose entries $(N_0, N_1, N_2, N_3, \ldots)$ are the number densities of hydrogen nuclei in all forms, $N_0 = n_p, N_1 = n_{1s}, N_2 = n_{2s}, N_3 = n_{2p}$, etc. In practice, the vector is truncated to some finite length $1 + \frac{1}{2} n_{max} (n_{max} + 1)$ by including only states with principal quantum number up to n_{max}. Including all atomic processes (bound-bound and bound-free), this vector evolves with time according to

$$\frac{d}{dt}\left(a^3 N\right) + a^3 C N = 0 \tag{4.8}$$

where $C(t)$ is a matrix. Conservation of protons implies $\sum_i C_{ij} = 0$, i.e. adding the rows of C gives zero. Note that $C_{io} = \alpha_i n_e$, the recombination rate to state i, is proportional to $n_e = n_p$. Thus Eqn. 4.8 is nonlinear. However, this nonlinearity

presents no diffuculties for the solution method that follows. The rates also depend on the photon occupation number, which must be separately specified. If the photon distribution is a blackbody, then the temperature $T(t)$ must be specified. Either way, Eqn. 4.8 must be integrated together with equations for other relevant quantities. Although the matrix C is not symmetric, it can be diagonalized by similarity transformation

$$C = -S\lambda S^{-1}, a^3 N = S\tilde{N}, \tag{4.9}$$

where

$$\lambda \equiv \text{diagonal}(0, \lambda_1, \lambda_2, \lambda_3, \ldots), \quad 0 < \Re(\lambda_1) \leq \Re(\lambda_2) \leq \Re(\lambda_1) \leq \ldots, \tag{4.10}$$

If S is unitary, then the eigenvalues should be real, but S is not unitary. We have to make sure mathematica, the program we will be solving our system with, allows for complex values. In practice, we found that while mathematica is able to find complex eigenvalues, all eigenvalues of S are real, so this is not a problem. As discussed before, there is always a zero mode, i.e., an eigenvector with eigenvalue 0, because C is a singular matrix. In practice, there is only one zero mode and the other eigenvalues are all real and negative (i.e. the evolution is damped and non-oscillatory). Using $\sum_i \sum_k C_{ik} S_{kj}$, it follow that $\sum_i S_{ij} = 0$ for $j \neq 0$. We are free to normalize the zero mode by $\sum_i S_{i0} = 1$. so that the zero-mode amplitude

$$\tilde{N_0} = a^3 \sum_i N_i = n_{0H} \tag{4.11}$$

is conserved and equals the mean number density of hydrogen nuclei in all forms today. We normalize all other eigenvectors by the condition

$$S_{0i} = 1 \text{ for } i \neq 0 \tag{4.12}$$

Substituting Eqn. 4.9 into Eqn. 4.8 gives

$$\frac{d\tilde{N}}{dt} + (\lambda + R)\tilde{N} = 0, \quad R = S^{-1}\frac{dS}{dt} \tag{4.13}$$

In practice, $R_{ij} \sim H$, i.e. the eigenvectors of C change with a characterisitc timescale of the Hubble time (the timescale for the photon and electron densities to change). On the other hand, λ^{-1} is typical of an atomic timescale, which for most or all nonzero eigenvalues is orders of magnitude shorter than the Hubble time. Thus, all fast modes quickly equilibrate with $\tilde{N}_i/n_{0H} \sim H/\lambda_i \ll 1$. In practice, for cosmological recombination at most one mode is slow to equilibrate, i.e. $H/\lambda_i \ll 1$ for $i > 1$. In this case, we can neglect $\tilde{N}_i$ for $i > 1$ and follow only one mode, $\tilde{N}_1$, in addition to the zero-mode. Eqn. 4.13 gives

$$\frac{d\tilde{N}_1}{dt} + (\lambda_1 R_{11})\tilde{N}_1 = -R_{10}\tilde{N}_0. \tag{4.14}$$

The formal solution of this equation, with initial conditions at t_0, is

$$\tilde{N}_1(t) = \tilde{N}_1 e^{-\mu(t_0,t)} - \tilde{N}_0 \int_{t_0}^{t} R_{10}(t') e^{-\mu(t',t)} dt'. \tag{4.15}$$

where

$$\mu(t_0, t) = \int_{t_0}^{t} [\lambda_1(t') + R_{11}(t')]\, dt'. \tag{4.16}$$

Eqn. 4.15 cannot be used without additional effort because the recombination rates C_{i0}, and therefore the rates R_{10} and R_{11}, depend on $n_e = n_p$ hence on $a^3 n_p = S_{10}\tilde{N}_0 + S_{11}\tilde{N}_1$. The equation is therefore a nonlinear integral equation. It is solved most easily by iteration.

1. Start at a sufficiently high temperature so that it is safe to assume $\tilde{N}_1 = 0$ (check $H/\lambda_1 \ll 1$) and $S_{i0} = 0$ for $i > 0$, hence $S_{00} = 1$. We begin our calculations at $z = 2000$, where $H/\lambda \sim 10^{-18}$. We run our simulation all the way to $z = 500$.
2. At time t, solve for n_e, using $a^3 n_e = S_{00} n_{0H} + \tilde{N}_1$. Using this n_e and the appropriate photon distribution, evaluate the matrix C_{ij}, its eigenvalues and eigenvectors. The results will be $S_{00} \neq 1$. Substitute back into $a^3 n_e = S_{00} n_{0H} + \tilde{N}_1$ with fixed $\tilde{N}_1(t)$ and iterate to convergence. The result will give the eigenvectors $S_{ij}(t)$ and eigenvalues $\lambda_i(t)$. Compute the inverse matrix $(S^{-1})_{ij}$.
3. Take a small timestep Δt so that a and the temperature change. With $\tilde{N}_1$ held

constant, repeat step 2 to obtain the eigenvectors and eigenvalues at time $t + \Delta t$. From these, estimate R_{10} and R_{11} at time $t + \frac{1}{2}\Delta t$ using

$$R_{1j} \approx \frac{1}{2\Delta t_k}[(S^{-1})_{1k}(t) + (S^{-1})_{1k}(t + \Delta t)][S_{kj}(t + \Delta t) - S_{kj}(t)]. \tag{4.17}$$

(Note that the sum over k starts at $k = 0$.) We use a time step of $z = 5$ converted to seconds by the Hubble time.

4. Use equation for one timestep to get a new estimate for $\tilde{N}_1(t + \Delta t)$:

$$\tilde{N}_1(t + \Delta t) = \tilde{N}_1(t)e^{-\mu} - (\frac{\tilde{N}_0 R_{10}}{\lambda_1 + R_{11}})(1 - e^{-\mu}), \mu = (\lambda_1 + R_{11})\Delta t, \tag{4.18}$$

where λ_1 is given by averaging $\lambda_1(t)$ and $\lambda_1(t + \Delta t)$ obtained from steps 2 and 3, respectively. With the procedure it is safe to take a stepsize large enough that $\mu \gg 1$ as long as $\lambda_1 + R_{11}$ and R_{10} change very little during the timestep.

5. Using this new estimate for $\tilde{N}_1(t + \Delta t)$, repeat steps 3 and 4. Iterate them until $\tilde{N}_1(t+\Delta t)$ converges. Save $\lambda_1(t+\Delta t)$, $S_{ij}(t+\Delta t)$ and $S^{-1}_{1k}(t+\Delta t)$; they can overwrite the previously stored values $\lambda_1(t)$, $S_{ij}(t)$ and $S^{-1}_{1k}(t)$.

6. Increment Δt and repeat steps 3-5. Continue through recombiantion.

The one level atom is instructive. With only one bound state, there is a single recombination rate $_e$ and photoionization rate β. Simple calculations give

$$\lambda_1 = \alpha n_e + \beta, \; R_{10} = \frac{d}{dt}(\frac{\beta}{\alpha n_e + \beta}), R_{11} = 0. \tag{4.19}$$

The solution depends on the interplay of three rates: αn_e, β, and H. At high redshift, B is the fastest rate leading to $x_p \equiv a^3 n_p / n_{0H} \approx 1$. As the temperate drops, αn_e becomes the fastest rate and x_p drops. Eventually H becomes the fastest rate and x_p freezes out at value around 10^{-3}. It is in this last stage that $\tilde{N}_1$ plays a crucial role. If only the zero mode is used, x_p decreases steadily instead of levelling off.

Chapter 5

Results

5.1 Overall Results

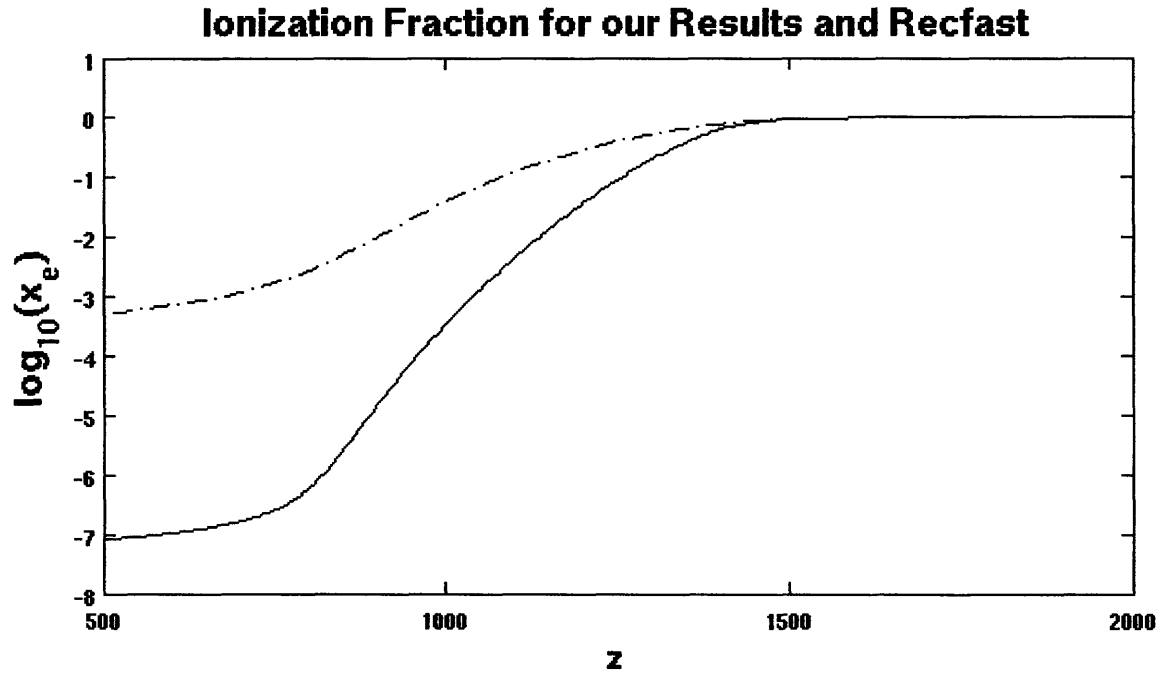

Figure 5-1: Our results (solid line) compared to the results of RECFAST (dashed line). Both plots show similar features: a break away from a fully ionized universe around $z = 1500$ and a levelling off around $z = 800$.

In figure 5.1, we see our final result for x_e compared with the result of RECFAST. We notice that for both results, the ionization fractions begin to break away from

1, or a fully ionized universe, around $z = 1500$. Our results show that the electron density drops very quickly and will recombine to form n_{1s}. There is a large disparity between our results and RECFAST, though. Our results seem to show that the effect of recombination is much stronger than RECFAST says it is. While we are not sure of the cause of this discrepancy, we can still proceed to analyze our results and in the meantime try to understand what the effects of our method are versus those of RECFAST.

5.2 Our method

The idea behind our iterative method is that we need not worry about modes that are much more rapid than the Hubble time. This factor can be expressed as λ/H. Each eigenvalue corresponds to a certain eigenvector, or mode, and if the eigenvalues are very fast, the corresponding process will go to equilibrium. In figure 5.2, we can see λ_1/H and λ_2/H from our C matrix. We notice that λ_2/H never drops below 10^{15}, while λ_1/H drops below 1 at $z \sim 1000$. When this happens, the effect of the addition of the one mode should kick in. Since λ_2 is not small, and our eigenvalues are ordered, we can understand that only λ_0 and λ_1 are not rapid and are significant.

Since λ_1 is greater than 1 till $z \sim 1000$, we should expect x_e when solving only with the 0-mode and x_e when solving with the addition of the 1-mode to remain close until $z \sim 1000$. This is what we see, as can be seen in Fig. 5.2. x_e would continue to decrease if it were not for the addition of the 1 mode. This addition causes the ionization fraction to steady out and then level off by 10^{-6}. Remembering Eqn. 4.18, we can understand this level at 10^{-6} because eventually as S_{00} drops low enough, then $\tilde{N}_1 > S_{00} n_{0H}$ and $\tilde{N}_1$ itself reaches about 10^{-13} or $10^{-6} \times n_{0H}$.

While the 1-mode is very important, the 0-mode still gives us some very crucial lessons about the populations of the various states. Fig. 5.2 shows S_{00}, S_{10}, S_{20} and S_{30}. Each one of these elements is a fraction of the total 0-mode proton population. We can see that S_{00}, corresponding to n_p, and S_{10}, corresponding to n_{1s}, make up the

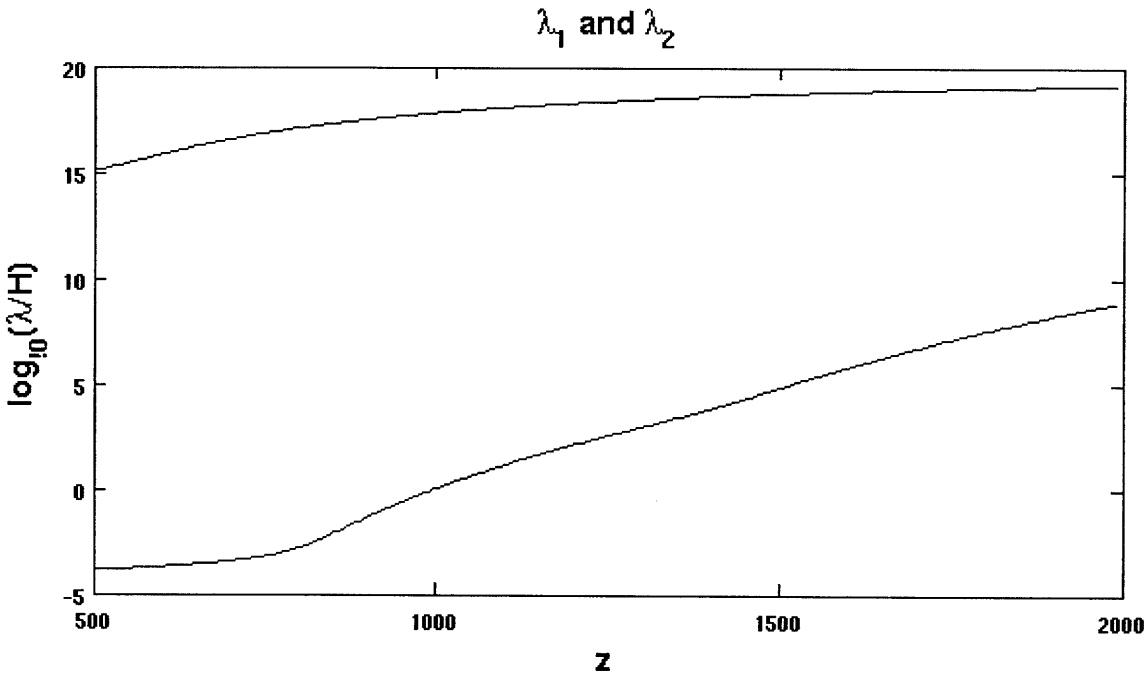

Figure 5-2: We show λ_1/H (bottom) and λ_2/H (top) of our C matrix evolving with time. The important thing to notice is that λ_1/H does fall below 1 at $z = 1000$.

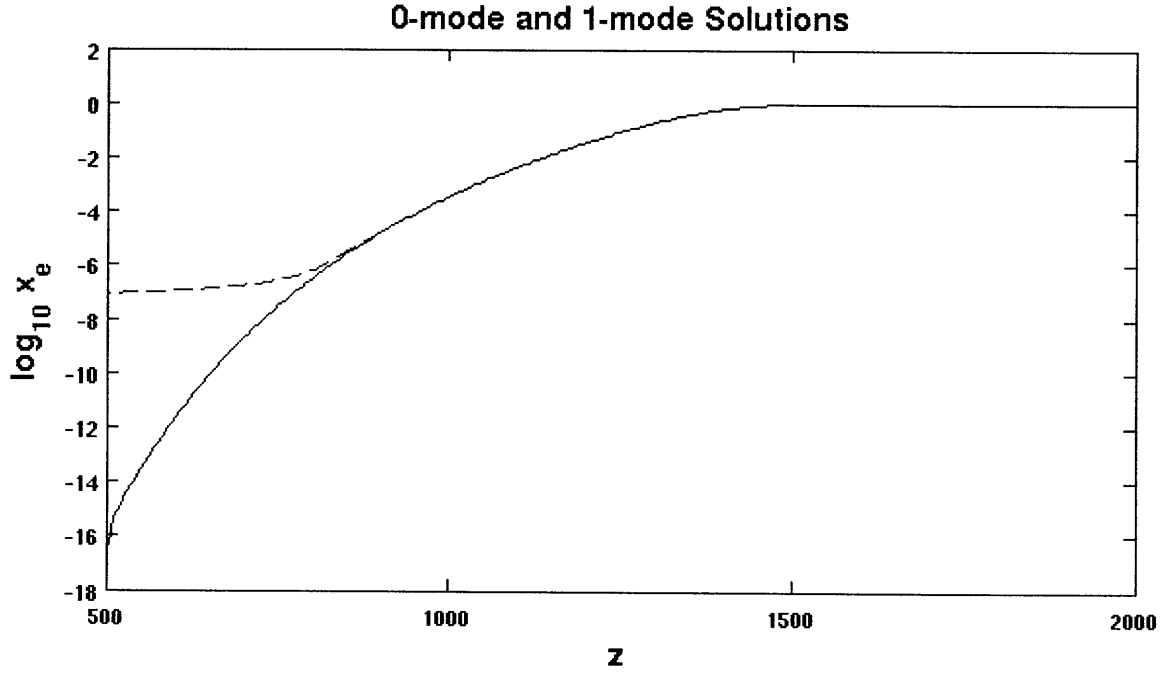

Figure 5-3: We see the 0-mode (solid) and 1-mode (dashed) solutions for x_e. We can see that adding in the 1-mode causes the 0-mode to level off.

bulk of the proton population. At $z \sim 1300$, n_{1s} grows larger than n_p. Interestingly, it is around this point that n_{2s} and n_{2p} are greatest. We also should note that n_{1s}, n_{2s} and n_{2p} all follow Peebles equilibrium assumption, given in Eqn. 3.36, very closely.

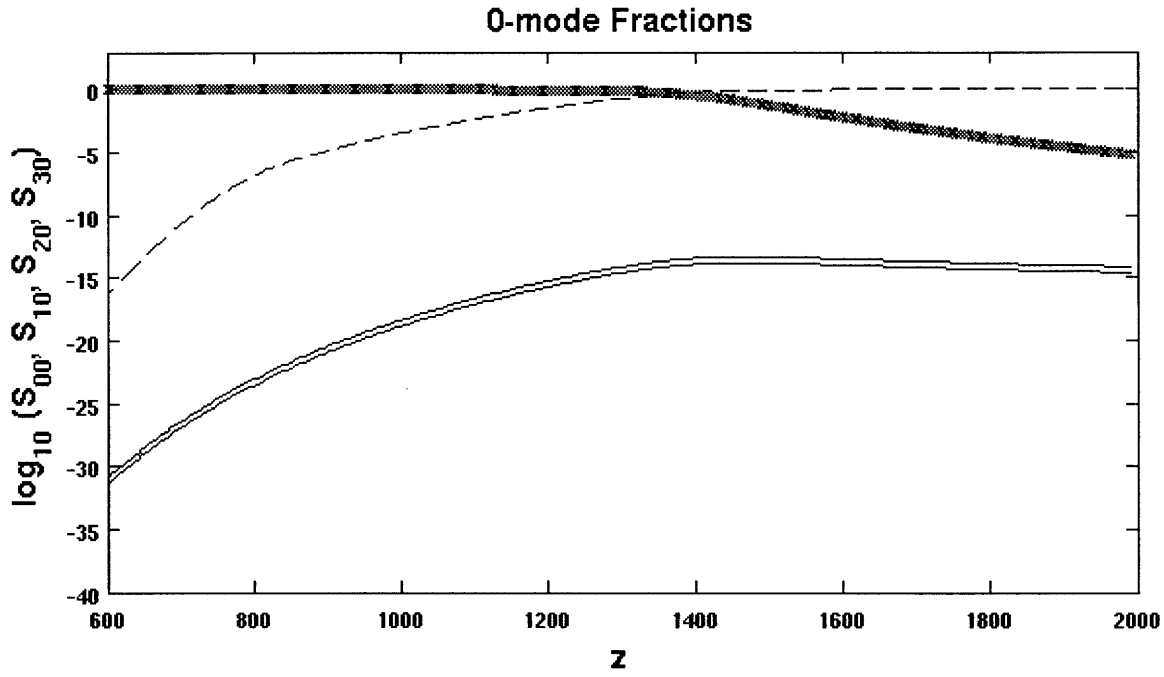

Figure 5-4: We see the 0-mode fractions for the states n_p (dashed), n_{1s}(' x '), n_{2s} (lower solid line), n_{2p} (higher solid line) corresponding to the S elements.

5.3 Understanding the effects of the various transitions

There are a couple ways we can understand the roles each transition plays during recombination. First, we can run our simulation with and without various processes, and second, we can compare different transition rates.

Let us first discuss the effect of changing our overall model of the atom. The results thus far include are for an atom with 22 levels, from n_{1s} all the way to n_{6f}. Now, we run our simulation with an atom that only goes up to $n = 4$. In Fig. 5.5, shown by 'x', we see that the difference between x_e in this model and the 6-level model reaches about a 4% difference at low redshift. Seager states that adding hundreds of

levels makes about an overall difference of 10%, so we can generally agree with this statement. We see though at higher redshifts, the difference is less than 1%, so until $z = 800$, there is hardly a difference. We also observe a dip at $z = 900$. While there is probably some reason for this, it is good to note now that there is a bit of inaccuracy due to our convergence. The convergence of our x_e values is 10^{-3}, so differences past this value must be taken lightly. We plot two other models on Fig. 5.3. Shown by the dashed line, we see the model assuming a case B recombination coefficient, or in other words, not including the photoionization from, or the recombination to, the n_{1s} state. We see that this has a 100% difference at $z = 600$ and fairly steadily climbs as z descends. Peebles makes the assumption that one can use a case B recombination coefficient, but this plot shows that at low redshift, there is a significant difference.

Lastly, by the solid line, we plot the model of the atom with no two photon decay from n_{2s} to n_{1s}. We see that the difference between this model and the model that includes this transition is very small.

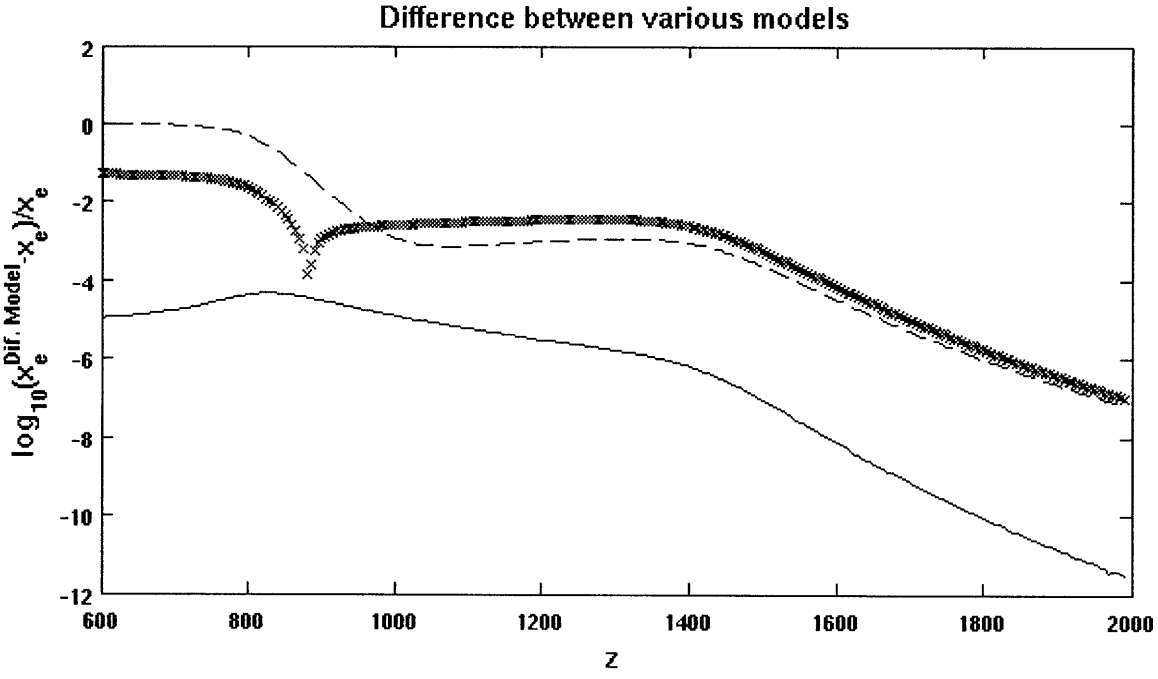

Figure 5-5: We show three different models of the atom. The 'x' shows a model with an atomic level maximum at $n = 4$. The dashed line shows a model assuming no photoionization from, or recombination to, the ground state and the solid line assumes there is no two photon decay.

To understand what are the significant factors in changing the ionization fraction, we look at the rates of various processes. In Fig. 5.6, we see the photoionization rates as well as the recombination rates as a result of our simulation. While the rates for recombination and photoionization to the n_{1s} are very close, the photoionization rate for n_{2s} and n_{2p} are much greater than the corresponding recombination rates. This would mean that any protons that recombine to form n_{2p} or n_{2s} would be immediately photoionized. However, there are other transitions that atom can make from the $n = 2$ states instead of photoionization. These transitions are spontaneous emission from n_{2p} and two photon decay from n_{2s}.

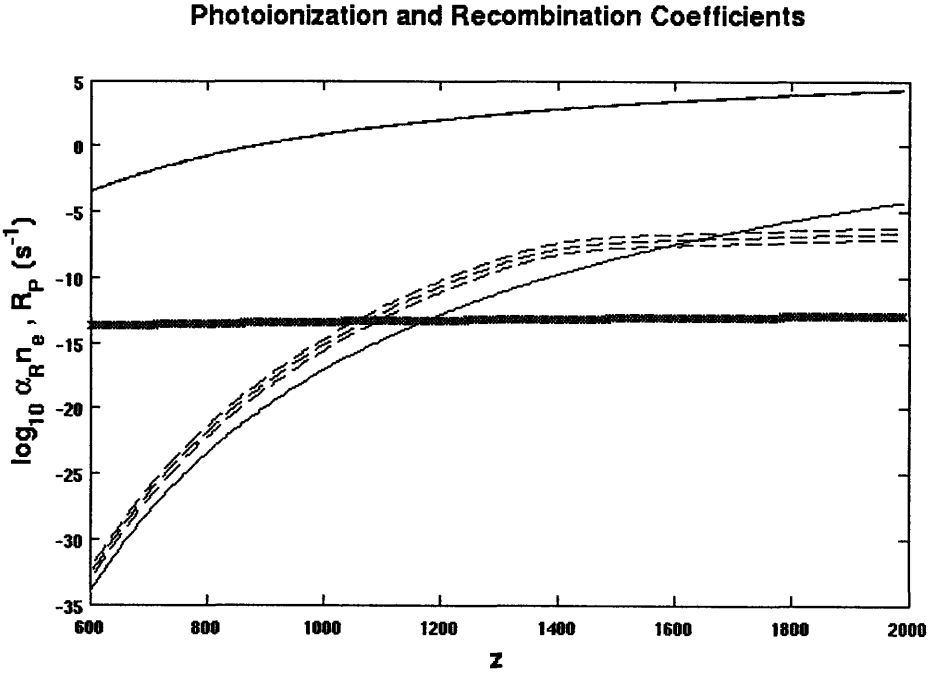

Figure 5-6: We show the recombination rates (dashed, with n_{1s} at top, followed by n_{2p} then n_{2s}), as well as the photoionization rates (solid), with n_{2p} and n_{2s} together at the top, and n_{1s} at the bottom, as well as the Hubble rate.

Instead of comparing rates, let us now compare the rate of transitions per unit volume, commonly called ΔR and in units of cm^{-3}. For example, for the spontaneous emission from n_{2p} to n_{1s}, we will plot $A_{21}(1+n_\gamma)n_{2p}$. Therefore, this rate of transitions will depend on the number of states to begin with. Let's focus on n_{1s} since this level ends up with all of the protons. Looking at a three-level effective atom, we have three

pairs of processes: photoionization/recombination, spontaneous emission/absorption and two photon decay (we have no inverse process for two photon decay). First then, let's plot the rate of transitions that cause n_{1s} to grow and then we will plot the total change of transitions between the inverse processes. We see this plot in Figure 5.7.

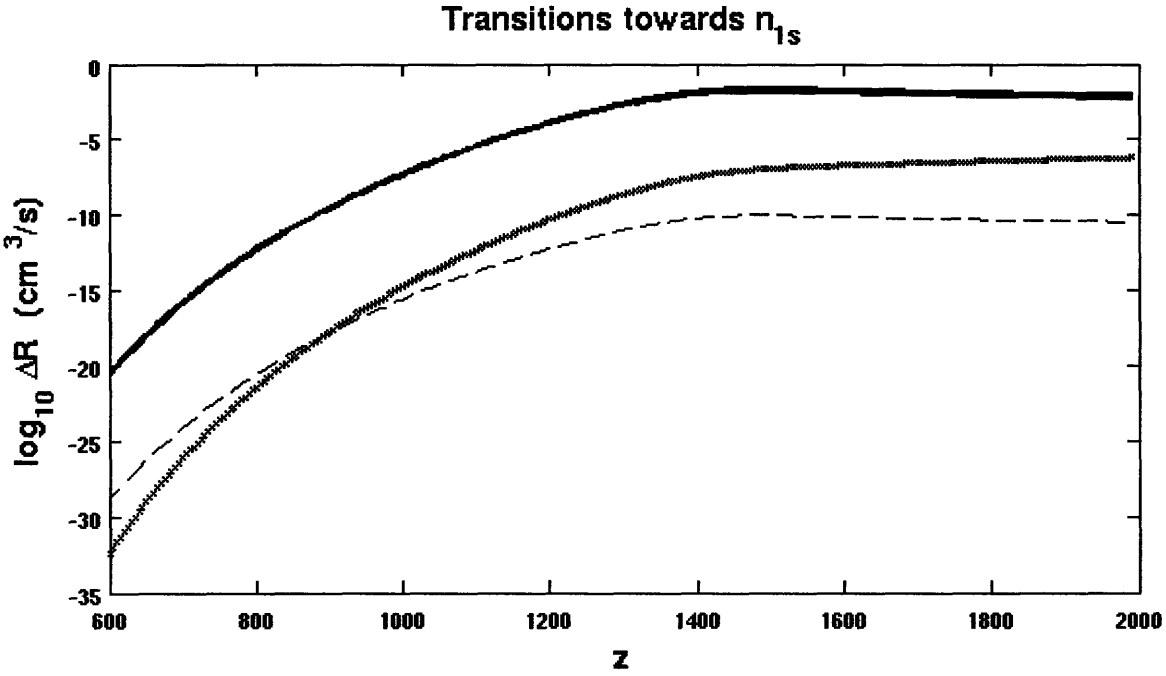

Figure 5-7: We show ΔR for recombination (denoted by 'x'), spontaneous emission from n_{2p} (solid line) and two photon decay from n_{2s} (dashed).

We see that most of the transitions occur from spontaneous emission from n_{2p} and the number of these transitions are about 10^6 greater than the transitions from n_{2s}. However, of more importance is the process between the pairs. While the rate of transitions from n_{2p} is very fast, it could mean very little if the rate from n_{1s} to n_{2p} is of equal magnitude. Therefore, we plot these three processes subtracted by their inverse processes in Fig. 5.8.

We can see that there is no contribution from $2p \leftrightarrow 1s$. This happens because the two processes, $A_{21}n_{2p}$ and $B_{12}n_{1s}$ reach equilibrium with each other and cancel each other out. This means that both of these rates must always be fast compared to the Hubble rate. We can see how this is true. A_{21} is of the order of 10^{-8} and while n_γ, the main factor of B_{12}, reaches 10^{-20} at low temperatures, B_{12} will still be fast compared

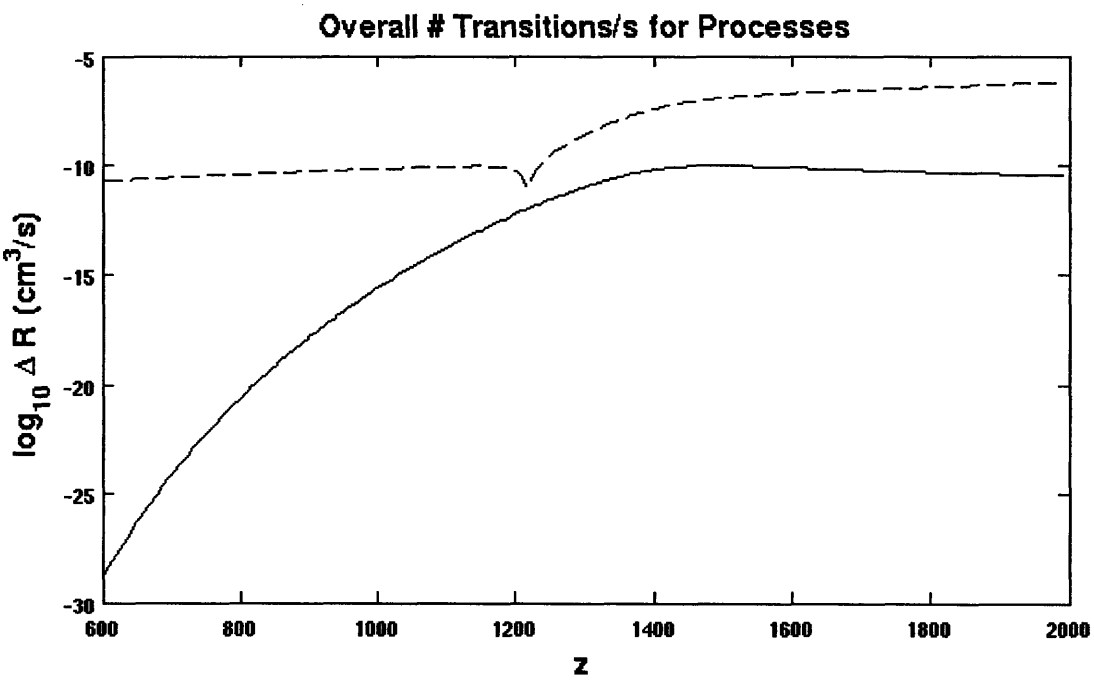

Figure 5-8: We show the magnitude of the process and its inverse for Photoionization/Rec. (dashed), $2s \leftrightarrow 1s$ (solid) and $2p \leftrightarrow 1s$ (not seen, since it is zero).

to the Hubble time because it is basically $A_{21}n_\gamma$. This way of looking at the processes may not always be right since we are multiplying the rate by the 0-mode population. The 0-mode population is not the exact population of all the states, and if we did use the whole population, we could see that this process falls out of equilibrium.

The two processes that we can clearly see have an effect are the recombination/photoionization as well as the two photon decay. We see that two photon decay has always a smaller effect than the greater amount of recombination than photoionization. This explains why when we took out two photon decay from our simulation, we only saw an error of 10^{-4}. This does not explain though why we don't see even more of an error when we use the Case B recombination coefficient. If recombination and photoionization to the ground state is important, then we should expect more of a difference (that being said, the difference did reach 100% at low redshift).

The underlying question we really want to answer is what are the main players that affect x_e. If we take out recombination to the ground state, then the only way to reach the ground state is from two photon decay or from the downward transition

of a p state. We can see that if this was true, the two photon decay would be the primary rate, which agrees with Peebles thinking.

We now return to the question of where we differ from RECFAST. Both Peebles and Seager state that two photon decay is the dominant rate because the lyman transitions go to equilibrium. We find that it is actually the recombination rate to the ground state that dominates. What does not make sense about this though is that when we take away this recombination, there is not that much of a difference. There must be some process at work, whether it is a problem in the routine or what not, that causes x_e to drop so quickly and therefore this is why we are not really seeing the effect of taking away two photon decay or recombination to the ground state.

Chapter 6

Future Work

Our original motivation for this was to study scattering effects of the photon spectrum on recombination. The two main processes that we would be looking at are Thomson scattering and resonance scattering. Once we have settled the method described in the focus of this paper, we will continue with our original goal.

6.0.1 The Sunyaev-Zel'dovich effect on the Frequency Spectrum

Our general method will be incorporating the various scattering effects into our calculations of the atomic transitions. For each z, we solve the atomic rate equations assuming a blackbody. This is an incorrect assumption. Certain processes will produce an abundancy of photons. For example, the two photon decay will produce photons that are not reabsorbed in the opposite reaction. This will cause a distortion to the blackbody. The blackbody, itself, will change due to the scattering effects. The Sunyaev-Zel'dovich effect, as we see here, will effectively take photons in and out of energy bins, thereby smoothing out the photon spectrum or causing further distortions.

The Sunyaev-Zel'dovich effect can be expressed by the Kompaneets equation:

$$\left(\frac{df}{dt}\right)_{SZ} = n_e \sigma_T \frac{1}{mE^2} \frac{d}{dE}\left[E^4\left(f\left(1+f\right)+kT_e\frac{df}{dE}\right)\right] \tag{6.1}$$

To understand the consequences of the Sunyaev-Zel'dovich effect, we will solve:

$$\frac{df}{dt} - HE\frac{df}{dE} = n_e\sigma_T \frac{1}{mE^2}\frac{d}{dE}\left[E^4\left(f\left(1+f\right) + kT_e\frac{df}{dE}\right)\right] \tag{6.2}$$

Using $x = \frac{E}{k_B T_\gamma (1+\Delta)}$

$$f = \frac{1}{e^x - 1} \tag{6.3}$$

$$\frac{df}{dx} = -f\left(1+f\right) \tag{6.4}$$

and therefore:

$$\frac{d\Delta}{dt} - \frac{\dot{a}}{a}E\frac{d\Delta}{dE} = \frac{(1+\Delta)^2}{f\left(1+f\right)}\frac{n_e\sigma_T}{mE^3}\frac{d}{dE}\left[E^4 f\left(1+f\right)\left(kT_\gamma - \frac{kT_e}{(1+\Delta)} + \frac{kT_e}{(1+\Delta)^2}E\frac{d\Delta}{dE}\right)\right] \tag{6.5}$$

For each time step, we will solve this equation, and use our new n_γ for all of our rate equations.

Chapter 7

Conclusions

In this paper, we carefully calculated the rates of various atomic transitions during recombination. We looked at bound-bound transitions, bound-free transitions and free-bound transitions. The difficulty in then solving all of these equations during recombination is the disparity of rates in the equations. When one solves differential equations, he must use a timescale equal to the fastest rate, but this rate is of the order of 10^8 and will take a very long time to solve since we need to span $\Delta z = 1500$. Our method bypasses this problem by creating rate matrices and only accounting for modes with a corresponding eigenvalue smaller than the Hubble time. We then iterate our value of x_e until convergence. Our results show what we should expect from recombination. Around $z = 1600$ the universe is no longer fully ionized and x_e continues to drop until $z = 800$ or so. The reason we are able to see this levelling off of x_e is through the addition of the 1-mode. There is a large difference between, though, between our results and the results of RECFAST. Our results show that recombination produces a much steeper decline of x_e than RECFAST does. We can understand the effects of the individual processes by eliminating that process from our simulation or look at the transition rates of the different processes. We used a 22-level atom (from n_{1s} to n_{6f}) for our simulations and compared different scenarios with the main one. We saw that taking away levels and only going to $n = 4$ changes x_e at low redshift by about 2%. We see that taking away two photon decay barely has any effect and taking away ground state recombination/photoionization causes

a significant change at low redshift. We were able to look at the transition rates of these processes to get a better idea of the effect each one is having. We saw that the lyman-alpha transition goes to equilibrium whereas the two photon decay continually produces n_{1s} states. We also saw that the difference between the recombination transitions and photoionization transitions to the ground states remains significant throughout recombination, and this could cause recombination to be much steeper than Seager explained it to be. However, when we take away this recombination, we see a similar effect, so we are forced to the conclusion that there is another factor involved that is making x_e drop like it does. Overall though, we are well on our way to solving this system of rate equations in an original way that allows us to understand the role of individual processes. After doing so, we will work on scattering effects of the photon spectrum. This project has been a great success in gathering a detailed understanding of recombination and should only get better in the near future.

Appendix A

References

Boardman, W.J., *Radiative Recombination Coefficients of the Hydrogen Atom*, Astrophys. J. Suppl, 9, 185, 1964.

Burgin, Kauts, and Shakhvorostova, *On the Effect of Collisional Transitions on the Cosmological Hydrogen Recombination Spectrum*, Astronomy Letters, 32, 8, 2006.

Menzel, D. H. and Pekeris, C. L. *Absorption Coefficients and Hydrogen Line Intensities* Monthly Not. Roy. Astron. Soc. 96, 77, 1935.

Mitchner M., Kruger Jr., *Partially Ionized Gases*, Wiley Series in Plasma Physics, 1992.

Omidvar K., McAllister, A.M., *Evaluation of high-level bound-bound and bound-continuum hydrogenic oscillator strengths by asymptotic expansion*, Phys. Rev. A 51, 1995.

Osterbrock D., Ferland G, Astrophysics of Gaseous Nebulae and Active Galactic Nuclei, University Science Books, 1989.

Peebles, P.J.E. *Recombination of the Primeval Plasma.* Astrophysical Journal, 153,1, 1968.

Peebles P.J.E., Principles of Physical Cosmology Princeton Univ. Press, 1993

Purcell, E.M., *The Lifetime of the* $2^2S_{1/2}$ *State if Hydrogen In an Ionized Atmosphere*

Scott D., Smoot G., *Cosmic Background Radiation Mini-Review* Physics Letters, B592, 1, 2004.

Seager S., Sasselov D., Scott D,*A New Calculation of the Recombination Epoch*, American Journal of Physics, 523, 1999.